SUPPLEMENTARY INFORMATION

SUSTAINED ENDOSOMAL RELEASE OF A NEUROKININ-1 RECEPTOR ANTAGONIST FROM NANOSTARS PROVIDES LONG-LASTING RELIEF OF CHRONIC PAIN

*Rocco Latorre[1,2], *Paulina D. Ramírez-Garcia[3], Alan Hegron[1,2], James L. Grace[3], Jeffri S. Retamal[3], Priyank Shenoy[3], Mai Tran[3], Luigi Aurelio[3], Bernard Flynn[3], Daniel P. Poole[3], Rafael Klein-Cloud[1,2], Dane D. Jensen[1,4], Thomas P. Davis[5], Brian L. Schmidt[1,2,4], John F. Quinn[3], Michael R. Whittaker[3], Nicholas A. Veldhuis[3,], Nigel W. Bunnett[1,2]

[1]Department of Molecular Pathobiology, New York University, New York 10010, USA
[2]Department of Neuroscience and Physiology, Neuroscience Institute, New York University, New York 10010, USA
[3]Monash Institute of Pharmaceutical Sciences, Monash University, Parkville, VIC 3052, Australia
[4]Bluestone Center for Clinical Research, New York University College of Dentistry, New York 10010, USA
[5]Australian Institute for Bioengineering and Nanotechnology, The University of Queensland, Brisbane, QLD 4072, Australia

* Equal first authors

Correspondence:
Nigel W. Bunnett, Ph.D., Department of Molecular Pathobiology, New York University, New York 10010, USA. nwb2@.nyu.edu
Nicholas A Veldhuis, Monash Institute of Pharmaceutical Sciences, 381 Royal Parade, Parkville, VIC 3052, Australia. nicholas.veldhuis@monash.edu
Michael R Whittaker, Monash Institute of Pharmaceutical Sciences, 381 Royal Parade, Parkville, VIC 3052, Australia. michael.whittaker@monash.edu

SUPPLEMENTARY FIGURES

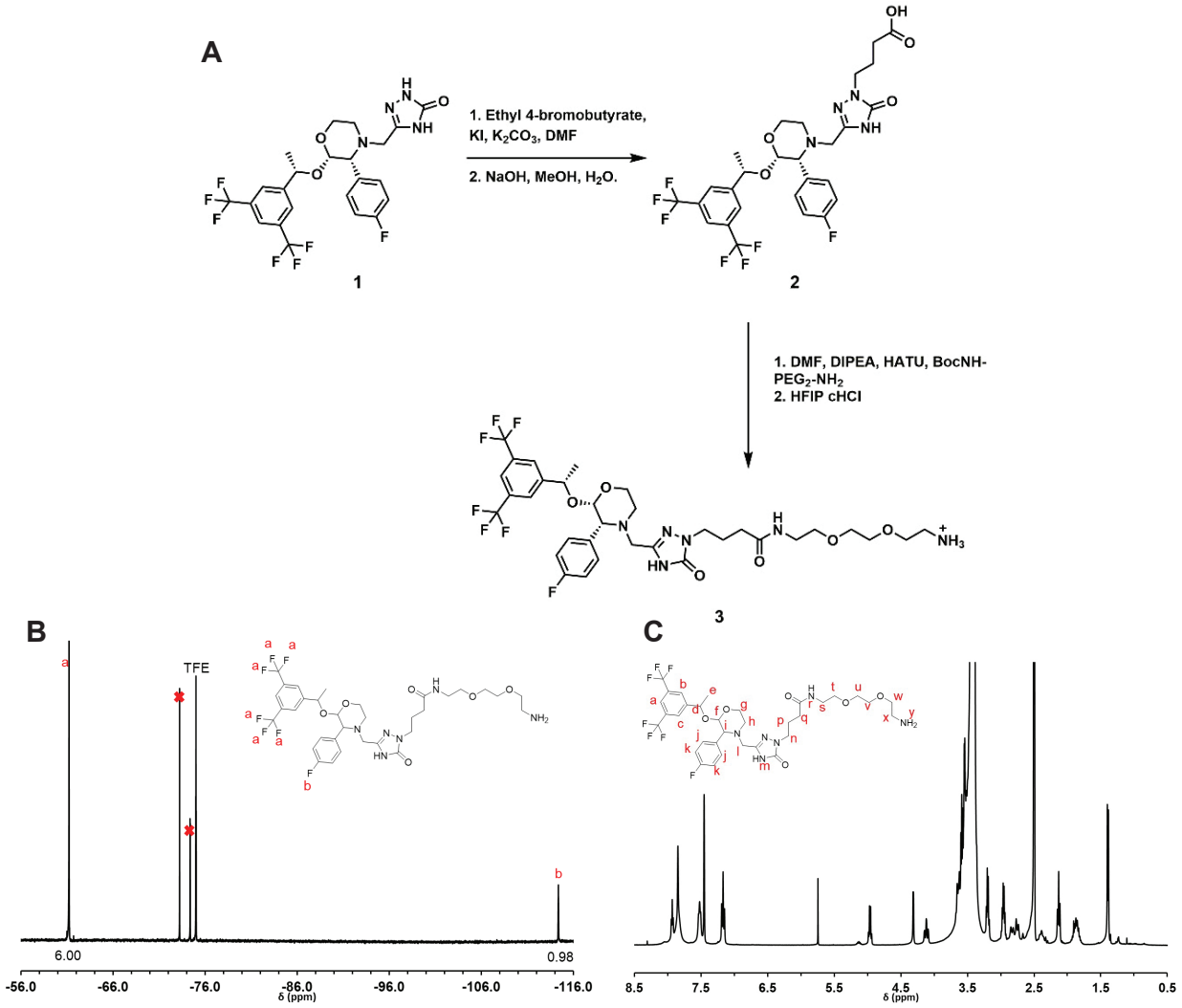

Figure S1. Synthesis and characterization of AP-NH_2. A. Synthetic scheme. AP-NH_2 comprised a 3-carbon linker and primary amine for conjugation to nanostar linker.**B.** ^{19}F-NMR of the starting material AP-NH_2. Red crosses (×) represent contaminant fluorine species in solution. **C.**^{1}H-NMR of the starting material AP-NH_2.

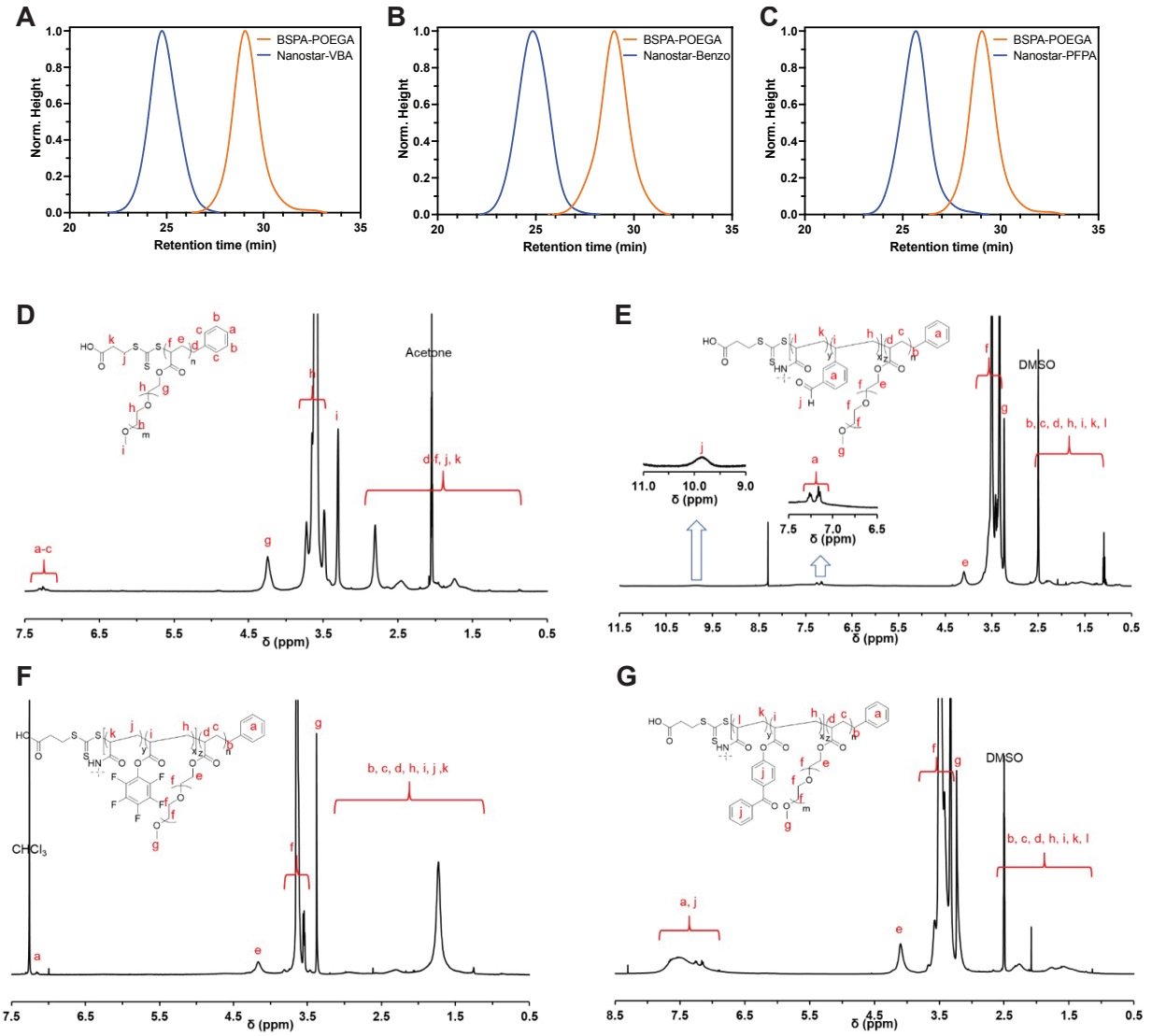

Figure S2. Characterization of nanostars. A-C. Evolution of molecular weight determined by GPC of the BSPA-POEGA arm polymer (orange) after star formation and purification (blue) with pentafluorophenyl acrylate (PFPA, **A**), 3-vinylbenzaldehyde (VBA, **B**) and 4-benzoylphenyl acrylate (Benzo, **C**). **D-G.** ^{1}H-NMR spectra of purified PEG arm (acetone-d6) (**D**), nanostar-PFPA ($CDCl_3$) (**E**), nanostar-VBA (DMSO-d6) (**F**) and nanostar-Benzo (DMSO-d6) (**G**).

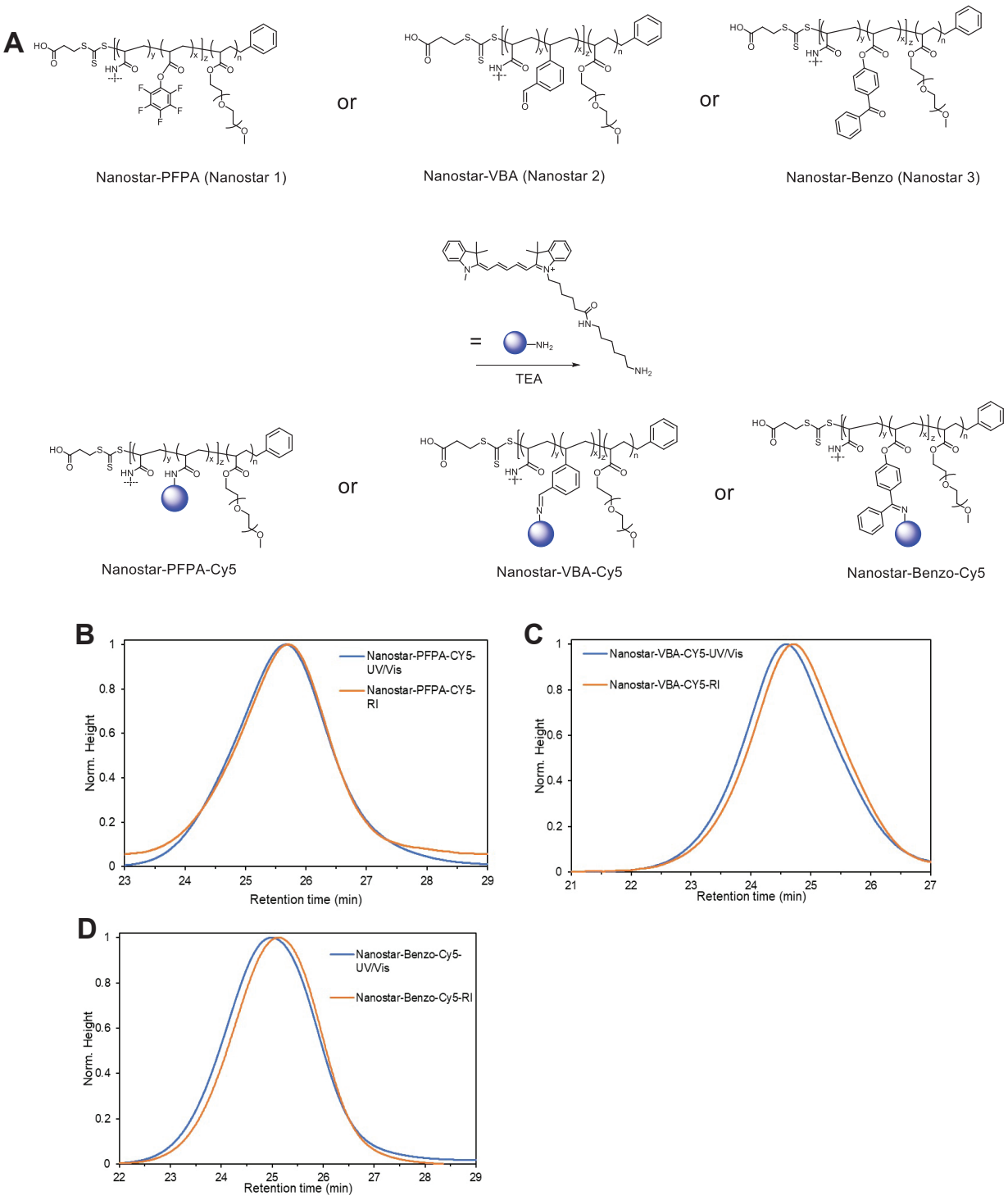

Figure S3. Synthesis and characterization of Cy5-labeled nanostars. A. Scheme for labeling of the nanostar polymers with Cy5-NH_2. **B-D.** GPC chromatograms with dual UV-Vis (λ = 646 nm, blue) and RI (orange) detection of nanostar-PFPA-Cy5 (**B**), nanostar-VBA-Cy5 (**C**) and nanostar-Benzo-Cy5 (**D**). Co-elution demonstrates effective labelling of the nanostars with Cy5. The slight shift in retention time for the UV-vis and dRI is due to arrangement of the detectors in series.

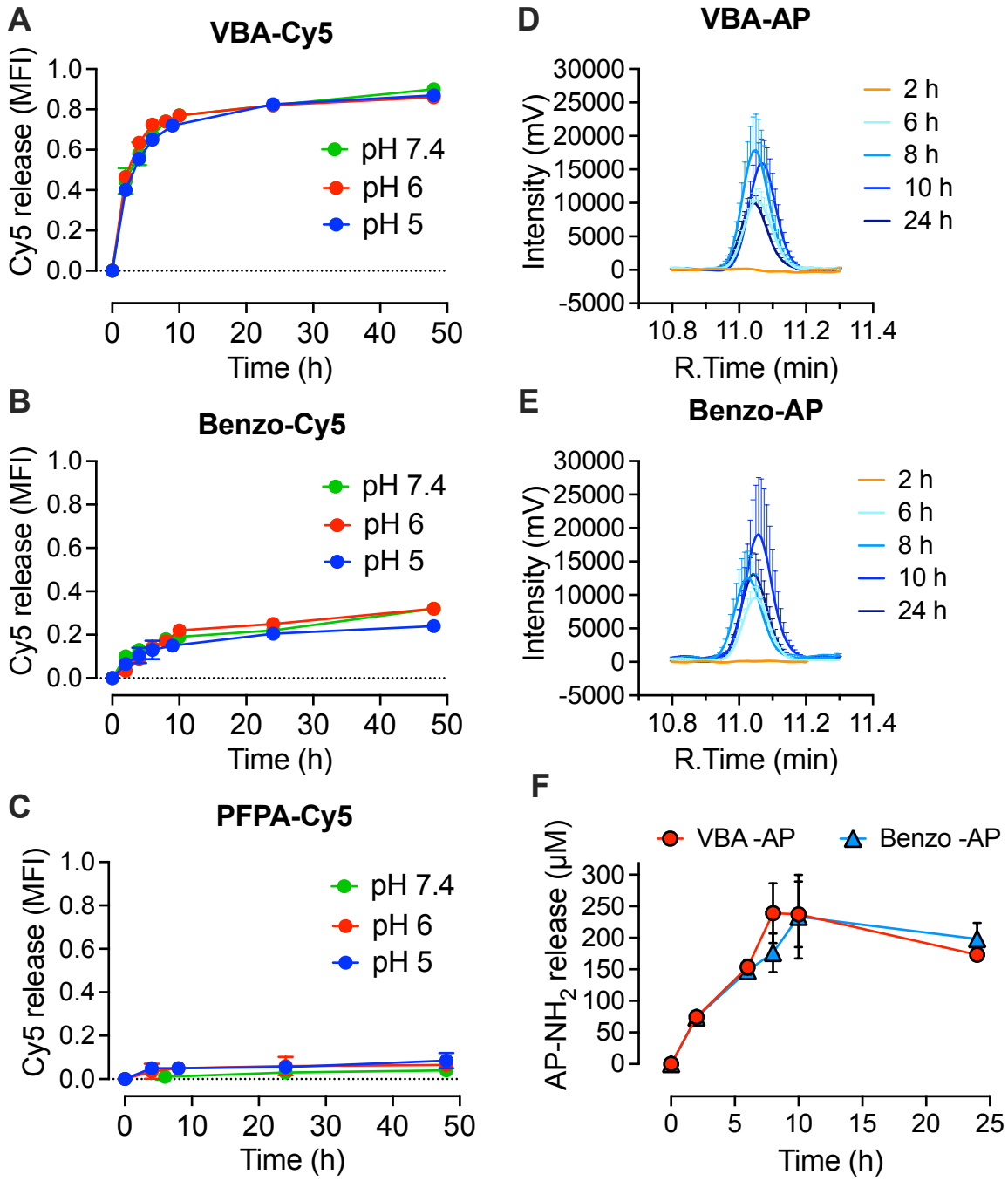

Figure S4. Profiling linker stability by release of Cy5-NH_2 and AP-NH_2 from nanostar-Cy5 and nanostar-AP conjugates. A-C. Release of Cy5-NH_2 was examined at pH 7.4, 6.0 or 5.0 over time. Cy5-NH_2 release was measured as mean fluorescence intensity (MFI, λ= 646 nm) for VBA-Cy5 (**A**), Benzo-Cy5 (**B**) and PFPA-Cy5 (**C**). Mean±SD, N=2-3 independent experiments. **D-F.** Release of AP-NH_2 was examined at pH 7.4 over time. AP-NH_2 release was assessed by HPLC. Chromatograms for AP-NH_2 release after 2, 6, 8, 10 or 24 h from VBA-AP (**D**) and Benzo-AP (**E**). **F** shows time course of AP-NH_2 release. Mean±SE, N=3 independent experiments.

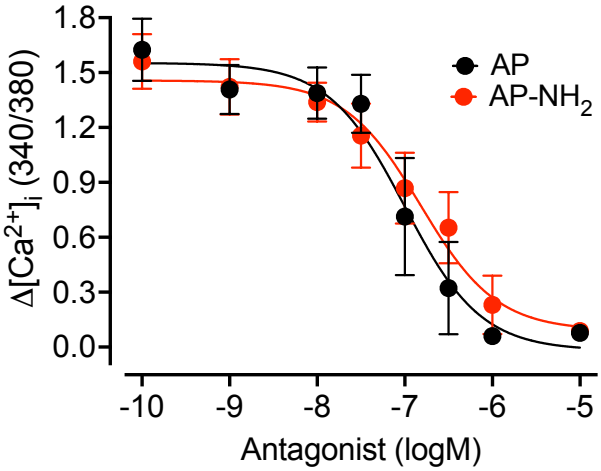

Figure S5. Antagonistic activity of AP-NH_2 and AP. Ca^{2+} transients were measured in HEK-NK_1R cells. Fura-2/AM loaded cells (2 µM, 45 min, 37°C, 5% CO_2) were pre-incubated for 30 min with increasing concentrations of AP or AP-NH2 before challenging cells with 10 nM SP (~EC_{80}). Data presented as mean±SEM of N=4 independent experiments performed in triplicate.

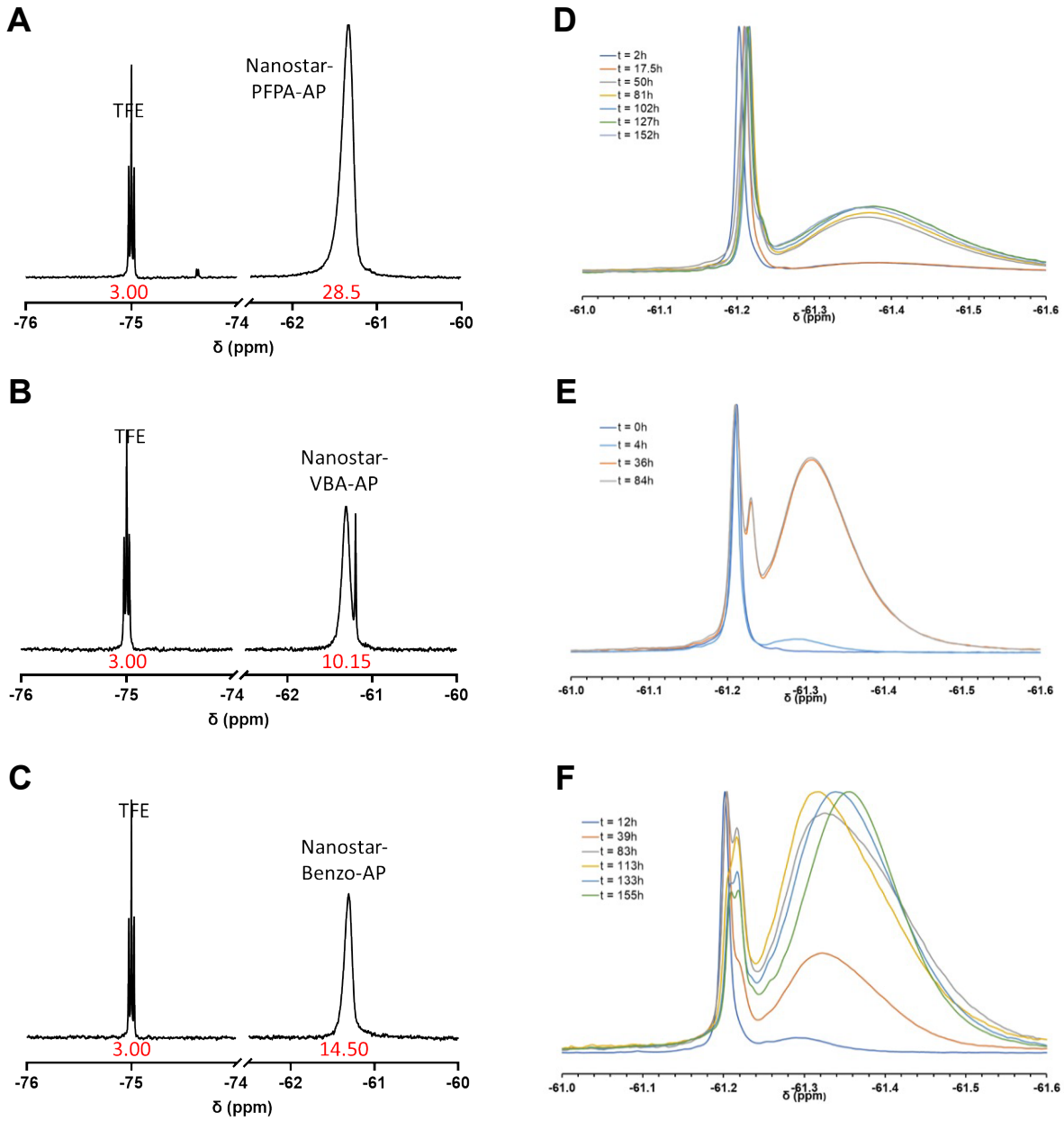

Figure S6. AP conjugation and release from nanostars. A-C. ^{19}F-NMR spectra of the purified AP conjugated to PFPA-AP (**A**), VBA-AP (**B**) and Benzo-AP (**C**). TFE (0.6 mM) was added as a standard. Samples were analyzed in DMSO-d6. **D-F.** Kinetic study of incorporation of AP-NH_2 into nanostars was assessed by ^{19}F-NMR spectra for PFPA-AP (**D**), VBA-AP (**E**) and Benzo-AP (**F**).

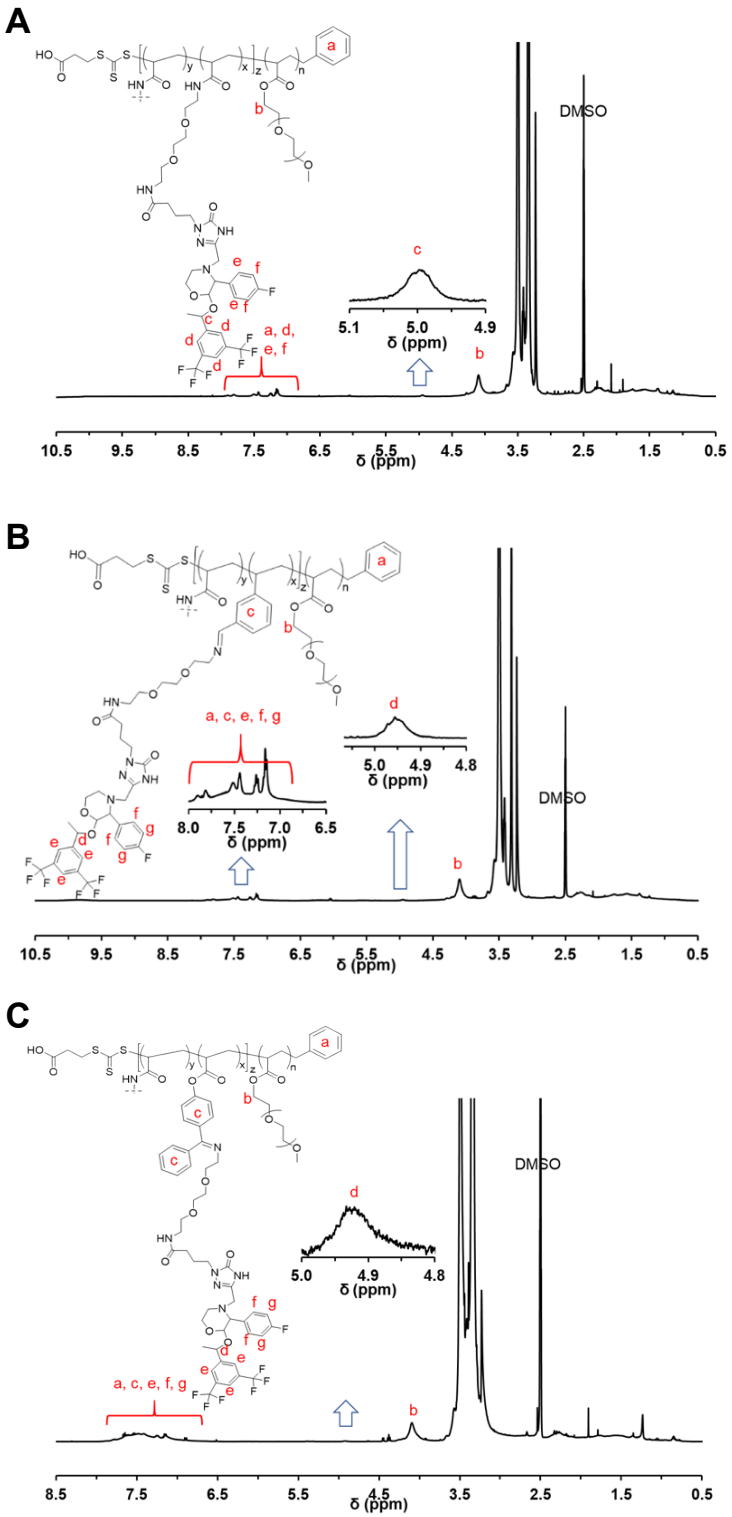

Figure S7. ^{1}H-NMR spectra of nanostars. Purified nanostar-PFPA-AP (**A**), nanostar-VBA-AP (**B**) and nanostar-Benzo-AP (**C**) in DMSO-d6. Characteristic proton assignments arising from the nanostar polymer scaffold and conjugated drug (AP-NH_2) are shown.

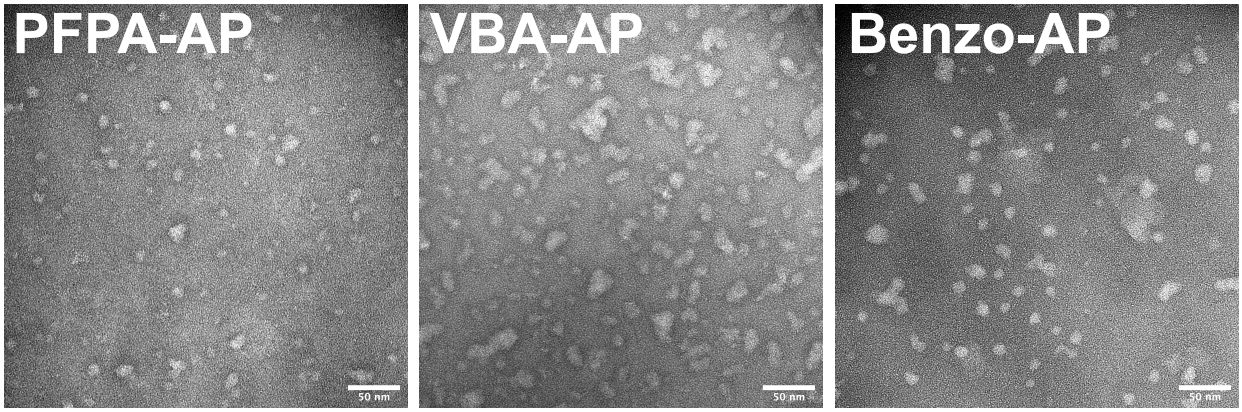

Figure S8. TEM of nanostars. Representative TEM images of PFPA, VBA and Benzo nanostars loaded with AP-NH_2. Scale bar=50 nm.

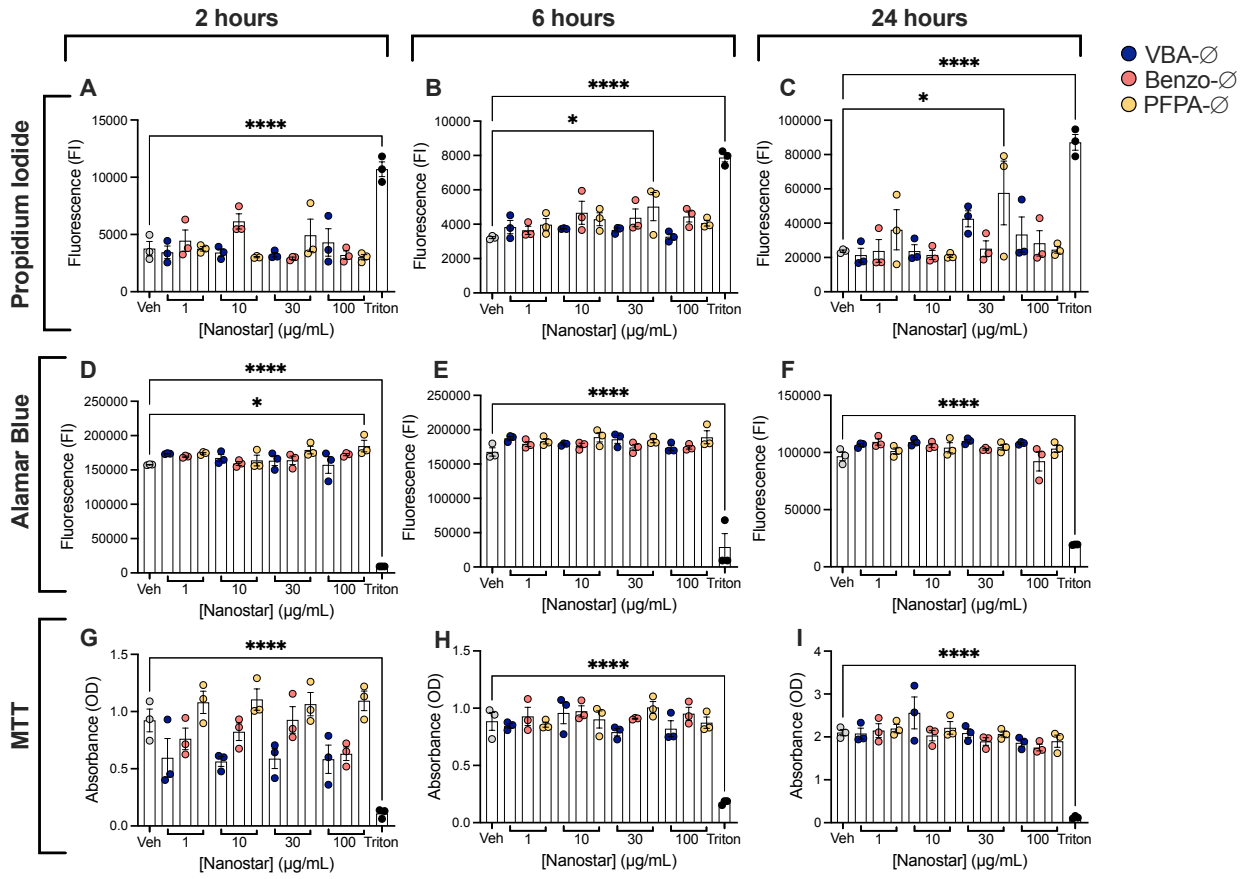

Figure S9. *In vitro* toxicity assessment of nanostars. VBA- Ø, Benzo-Ø and PFPA-Ø (1-100 µg/ml) were incubated for 2, 6 and 24 h with HEK293 cells. Propidium iodide was used to assess plasma membrane integrity (**A-C**), Alamar Blue was used to assess redox activity (**D-F**) and Thiazolyl Blue Tetrazolium Bromide (MTT) was used to assess mitochondrial activity (**G-H**). Mean±SEM. N =3 independent experiments. One-way ANOVA, Dunnett's multiple comparisons test, compared to vehicle. **** P<0.0001, *P=0.332.

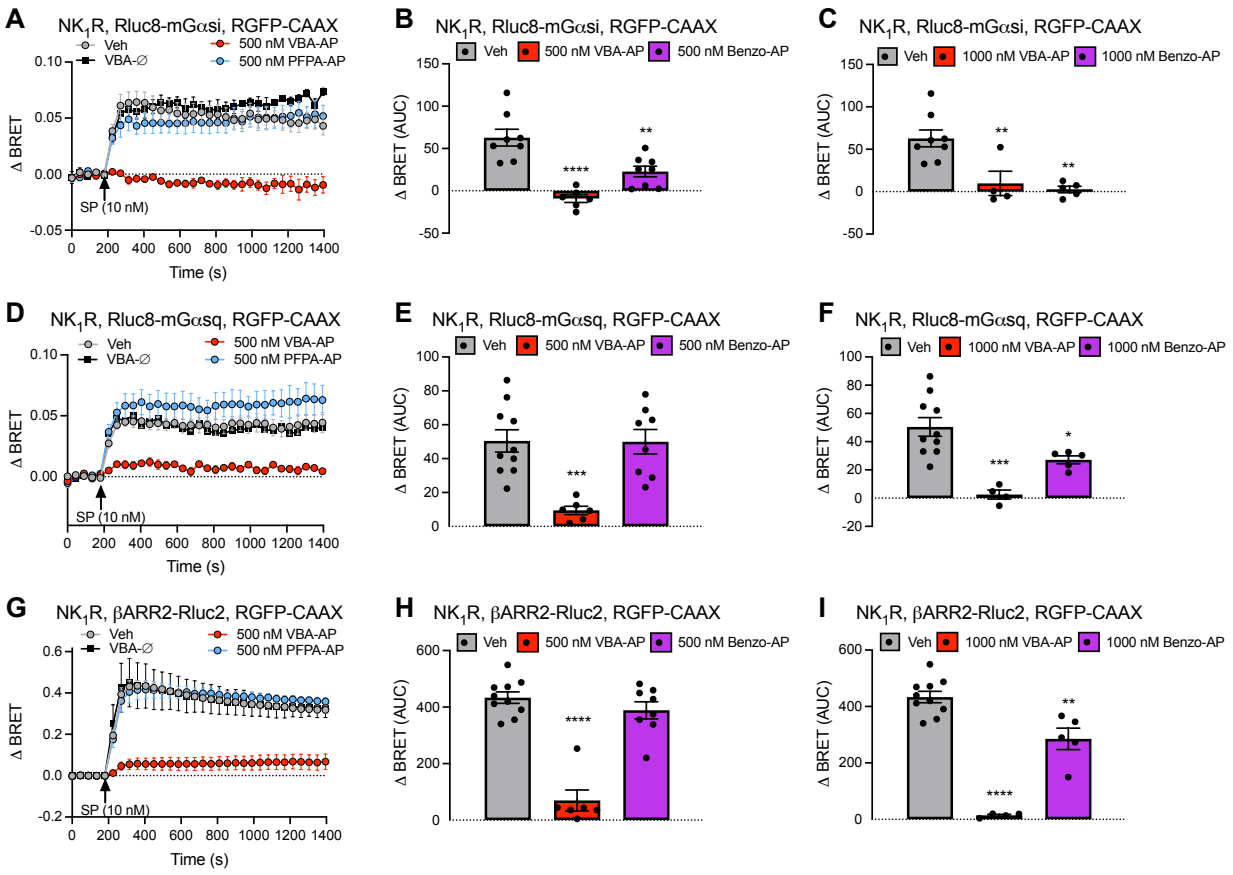

Figure S10. Nanoparticles and plasma membrane NK_1R signaling in HEK293T cells. Effects of SP (10 nM) on EbBRET between Rluc8-mGα_{si} (**A, B, C**), Rluc8-mGα_{sq} (**D, E, F**) and βARR2-Rluc2 (**G, H, I**) with RGFP-CAAX. Cells were preincubated with vehicle (Veh, control), VBA-AP, Benzo-AP, PFPA-AP (500 nM AP loaded in nanoparticles: **A, B, D, E, G, H**; 1000 nM AP loaded in nanoparticles: **C, F, I**) or VBA-Ø for 4 h before stimulation with SP and measurement of EbBRET. **A, D, G**: time course of EbBRET prior and after SP (10 nM) stimulation. **B, C, E, F, H, I**: area under the curves (AUC) of corresponding time course of EbBRET. Mean±SEM. N=3-10 independent experiments. **P*<0.05, ***P*<0.001, ****P*<0.001, *****P*<0.0001. One-way ANOVA, Dunnett's multiple comparisons test.

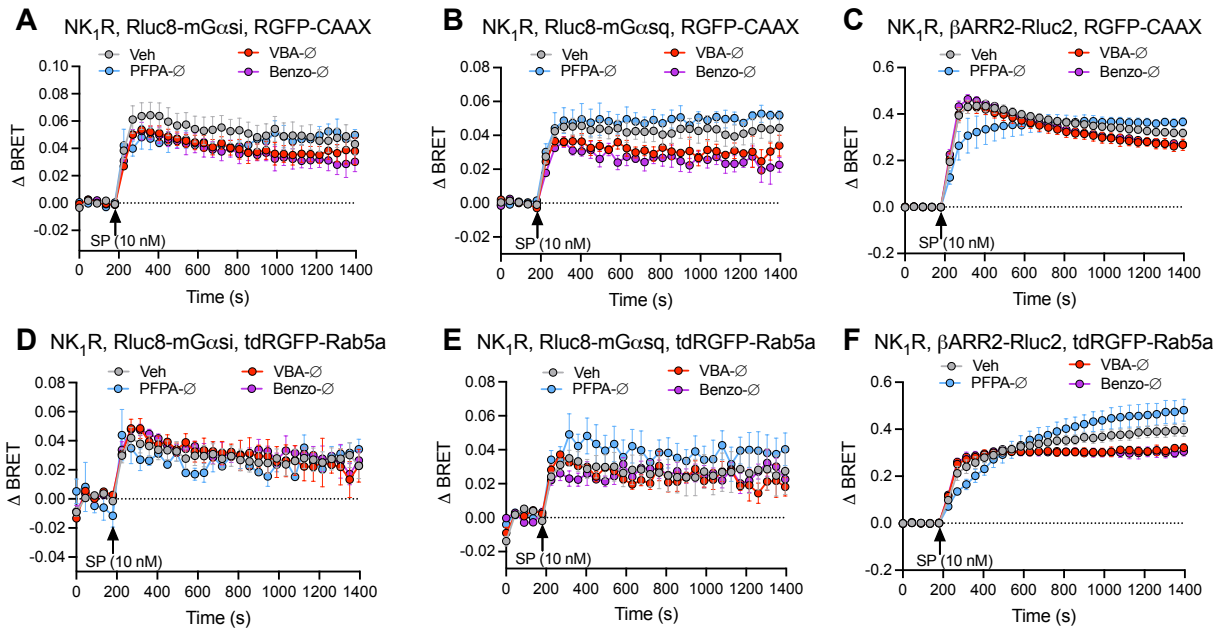

Figure S11. Empty nanoparticles and NK_1R signaling in HEK293T cells. Effects of SP (10 nM) on EbBRET between Rluc8-mGα_{si} (**A, D**), Rluc8-mGα_{sq} (**B, E**) and βARR2-Rluc2 (**C, F**) with RGFP-CAAX (**A, B, C**) or tdRGFP-Rab5a (**D, E, F**). Cells were preincubated with vehicle (Veh), VBA-Ø, Benzo-Ø or PFPA-Ø for 4 h before stimulation with SP and measurement of EbBRET. Curves represent time course of EbBRET prior and after SP (10 nM) stimulation. Mean±SEM. N=3-10 independent experiments.